Journal of Lasers in Medical Sciences

J Lasers Med Sci 2022;13:e24

Original Article

http://journals.sbmu.ac.ir/jlms

doi 10.34172/jlms.2022.24

Myocardial Ischemia Detection by a Sensitive Pump-Probe Atomic Magnetometer

Amin Zamani[1], Maliheh Ranjbaran[2], Mohammad Mehdi Tehranchi[1,3*], Seyedeh Mehri Hamidi[1], Seyed Mohammad Hosein Khalkhali[4]

[1]Laser and Plasma Research Institute, Shahid Beheshti University, Tehran, Iran
[2]Department of Physics, Central Tehran Branch, Islamic Azad University, Tehran, Iran
[3]Physics Department, Shahid Beheshti University, Tehran, Iran
[4]Physics Department, Kharazmi University, Tehran, Iran

***Correspondence to**
Mohammad Mehdi Tehranchi, Laser and Plasma Research Institute, Shahid Beheshti University (SBU), Velenjak Street, Tehran, Iran.
Tel: +982144600280;
Email: teranchi@sbu.ac.ir

Received: August 5, 2021
Accepted: December 21, 2021
Published online May 26, 2022

Abstract

Introduction: Magnetocardiography (MCG) based on optical atomic magnetometers has shown promise for detecting heart diseases accurately. Different methods were introduced to improve the sensitivity of detecting magnetic fields during cardiac activity.

Methods: In this paper, an optical pump-probe magnetometer operated on the ground-state Hanle effect based on the zero-field level crossing technique was developed and the laser output signal was optimized in an unshielded environment. Then, the optical magnetometer was utilized to record the simulated MCG trace of different stages of myocardial ischemia.

Results: The probe output light intensity followed the variation of cardiac magnetic field (MCG trace) generated by Helmholtz coil accurately.

Conclusion: Based on the results, the feasibility of our highly sensitive optical magnetometer in tracing showed no change in the P-QRS-T waveform associated with ischemic heart disease (IHD), where P indicates atrial depolarization, QRS is responsible for ventricular depolarization, and T represents ventricular repolarization.

Keywords: Magnetocardiography (MCG), Myocardial ischemia, Optical atomic magnetometer, MCG trace, Hanle effect

Introduction

Nowadays, human biomagnetism has attracted a lot of attention in research and medicine. The interest in using biomagnetism for studying ischemic heart disease (IHD), as one of the most serious diseases, has increased recently regarding the statistics related to mortality and incidence. IHD is considered a major concern around the world and the detection of myocardial ischemia remains to be a challenge in cardiological diagnosis.[1,2] Myocardial ischemia occurs due to a reduction in blood supply to the heart, leading to a decrease in blood oxygen, causing abnormal repolarization and excitation of wave conduction patterns in the tissue described in cardiac arrhythmias which are recorded with cardiography devices.[3] Therefore, a fast, accurate, highly sensitive, and noninvasive instrument is required for diagnosing IHD disease.

Intra- and extracellular ionic activity in cardiac muscle (myocardium) generates electrical potentials on the body surface area, and this electric current flowing through the heart leads to a magnetic field surrounding the source of the current[1]. Some studies have shown that magnetocardiography (MCG) can provide useful complementary or unique information about heart diseases, such as a tracing of the heart electromagnetic activity. The MCG signal (P-QRS-T complex) is used for diagnosing the heart condition, while the tracing path is the distance taken up by the impulses in the heart muscles. The patterns obtained from the patients with cardiac arrhythmias like myocardial ischemia offer substantial information related to P, QRS, and T heart features.[4] In these features, the P wave is related to the depolarization (activation) of the left and right atrium, the QRS complex of which is produced by the atrioventricular node (AV) including the Q, R, and S waves related to ventricular depolarization. The T wave following the QRS complex indicates ventricular repolarization.

Baule et al introduced the magnetic field produced by the heart and recorded the MCG trace of a human heart by means of a pair of pick-up coils, and superconducting quantum interference devices (SQUIDs), very sensitive magnetometers used to measure extremely subtle magnetic fields based on superconducting loops containing Josephson junctions, have taken the place since then.[5,6] SQUIDs have achieved a noise limit of about $1fT/\sqrt{Hz}$ 7, but they usually operate in arrays of multichannel matched

Please cite this article as follows: Zamani A, Ranjbaran M, Tehranchi MM, Hamidi SM, Khalkhali SMH. Myocardial ischemia detection by a sensitive pump-probe atomic magnetometer. *J Lasers Med Sci.* 2022;13:e24. doi:10.34172/jlms.2022.24.

gradiometers, and the cost and cryogenic working temperature are considered as the weaknesses of these devices. In recent years, atomic magnetometers known as optically pumped magnetometers (OPMs) have replaced other MCG devices due to some advantages such as low cost, high sensitivity comparable to SQUIDs, and working at room temperature.[8-10] OPMs are based on the Larmor precession of atoms with nonzero angular momentum in a magnetic field.[11] Atomic magnetometers showing sensitivities up to several $aT/\sqrt{Hz}$ [12] and presenting a non-invasive method can be implemented in detecting and localizing heart diseases like myocardial ischemia.[13,14]

In this paper, an atomic magnetometer was presented based on a Hanle effect method, which is appropriate for biomagnetic applications in an unshielded environment. The system was calibrated and the characteristics of the magnetometer were optimized by compensating the Earth's magnetic field to near-zero condition. Then, a normal MCG trace of the human heart and different modes of myocardial ischemia were simulated through Helmholtz coils and measured by the pump-probe atomic magnetometer.

Materials and Methods

Experimental Setup

The experimental setup is shown in Figure 1. The core of the optical magnetometer was a cylindrical cell containing rubidium atoms (^{85}Rb and ^{87}Rb) with 50 mm length and 25 mm diameter. 10 torr N_2 gas was filled in the cell to quench the Rb excited atoms, and the cell walls were coated by octadecyltrichlorosilane to reduce the spin destruction from wall collisions. Then, the cell was heated electrically utilizing a resistive wire to obtain sufficient Rb vapor density. A distributed feedback diode laser tuned to the D_1 resonance of rubidium at 794.8 nm was used for optical pumping and probing. A beam splitter split the laser beam with a diameter of 3 mm into two portions. The first portion was circularly polarized to pump the atoms optically, and the precession of the associated atomic spin in the presence of a magnetic field was detected by measuring the optical rotation of the linearly polarized light as the second portion, as shown by the dotted line in Figure 1. The power densities of the pump and probe beam were 3.5 and 160 μW/cm^2 respectively. An optical chopper was used to modulate the probe beam with a frequency of 170 Hz. Another linear polarizer adjusted the amplitude of beams in the probe direction.

The light passed through the vapor cell split into S- and P-polarized beams using a Wollaston prism. Then, the beams were captured by large area photodetectors, and the magneto-optical Faraday effect was observed by differential measurement of the perpendicular components of the probe light. For this purpose, a lock-in amplifier recorded the subtraction of S and P components which altered by applying the cardiac magnetic field. This differential method, which is based on the phase-sensitive detection performed by the lock-in amplifier, enhanced the signal-to-noise ratio and measurement sensitivity. In the next procedure, the outputs of photodetectors were fed into the channels of the oscilloscope for monitoring the intensity of the pump and probe beams against the applied cardiac magnetic field.

Further, three orthogonal pairs of Helmholtz coils were used for compensating the Earth's magnetic field via applying opposite fields in each direction, and consequently, the magnetic field was held near zero.

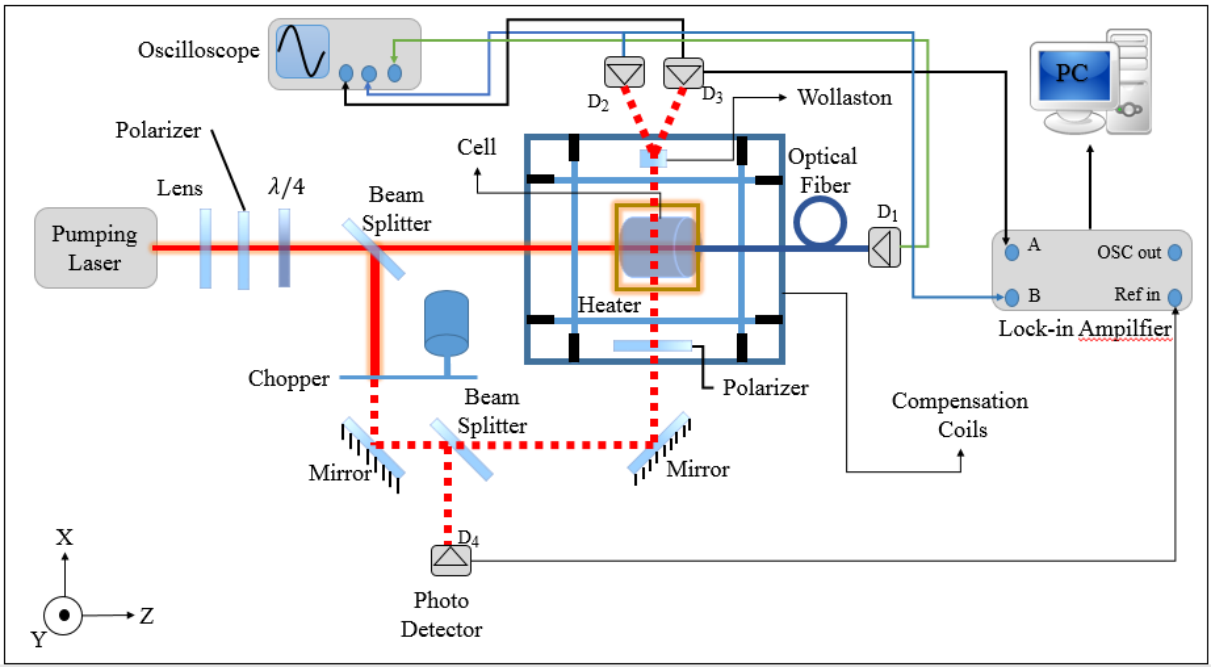

Figure 1. Experimental Setup.

As it was already mentioned, our experimental setup should be characterized and calibrated in the vicinity of the zero magnetic field. In the first step of compensation, a Hall sensor was used for measuring three components of the earth's magnetic field. Then, opposite currents were applied to 3D Helmholtz coils for compensating the earth's field to about 1 μT by using a programmable DC power supply. In the next step, the atomic magnetometer was utilized to compensate the remaining magnetic field to ~100nT. Finally, the process of calibrating the measurement setup decreased the background magnetic field to ~20nT, as described below.

Calibration of the Magnetometer

As shown in Figure 2a, the variation of the in-phase component of the lock-in amplifier was registered by applying the magnetic field by transverse coils and monitoring the output of photodetectors in the probe direction. The following equations show the evolution of longitudinal and transverse polarization components of probe light:

$$P_z = P_0 \frac{\Delta B^2}{B_y^2 + \Delta B^2}$$

$$P_x = -P_0 \frac{B_y \Delta B}{B_y^2 + \Delta B^2}$$

As displayed in Figure 1, the direction of the pump beam lay along the z axis and the magnetic field was applied along the y axis, as well as ΔB=Γ/γ and $P_0 = \frac{R_{op}}{R_{rel}}$. Thus, the intensity variation along z direction was proportional to P_z. As estimated in the above equations, the curve has an inflection point crossing the zero point and is a derivative of the Lorentzian curve (P_x).

The output signal of photodetectors in probe direction (D_1 and D_2) confirmed that the perpendicular components of polarization behaved in an opposite direction and the differential method increased the sensitivity.

In the next step, the longitudinal magnetic field was swept, and the amplitude and phase of the output signal in differential mode were recorded. As shown in Figure 2b, the minimum point of the amplitude curve defines the residual magnetic field in longitudinal (pumping) direction such as B=16.58nT in Figure 2b. One can compensate the magnetic field at the cell location by applying the residual magnetic field by additional Helmholtz coils in appropriate direction.

The Hanle effect method which is based on the magnetic field sweeping and output intensity monitoring in longitudinal and transverse directions was used for zero field finding process. The amplitude and line width vary in longitudinal direction (z) as follows:

$$A_{\parallel}(\omega_{\perp}) = \kappa_0^{unpol} L P_0 \frac{\omega_{\perp}^2}{\omega_{\perp}^2 + \gamma_1\gamma_2}, \qquad \gamma_{\parallel}(\omega_{\perp}) = \sqrt{\gamma_2^2 + \frac{\gamma_2}{\gamma_1}\omega_{\perp}^2}$$

where $\omega_{\perp}$ is the corresponding Larmor frequency of the transverse magnetic field, and γ_1 and γ_2 are longitudinal and transverse relaxation rates respectively. Based on the equations, the amplitude of the longitudinal Hanle effect is proportional to the magnitude of the applied transverse magnetic field. Both amplitude and line width of the longitudinal Hanle curve increase with the transverse magnetic field. Therefore, the zero crossing point was determined by finding the minimum amplitude and line width. The minimum line width of the longitudinal Hanle curve achieved in the zero transverse magnetic field is equal to γ_2 and it is about γ_2=400 Hz for our present Rb cell.

The transverse Hanle effect was studied by sweeping the transverse magnetic field and recording the amplitude and phase of the output signal in differential mode. These components change based on the following equations:

$$A_{\perp}(\omega_{\parallel}) = \kappa_0^{unpol} L P_0 \qquad , \qquad \gamma_{\perp}(\omega_{\parallel}) = \sqrt{\gamma_1\gamma_2 + \frac{\gamma_1}{\gamma_2}\omega_{\parallel}^2}$$

The amplitude of the Hanle curve is not dependent on the longitudinal magnetic field. Thus, it cannot be used to null the longitudinal magnetic field.

The amplitude of the output signal can be recorded

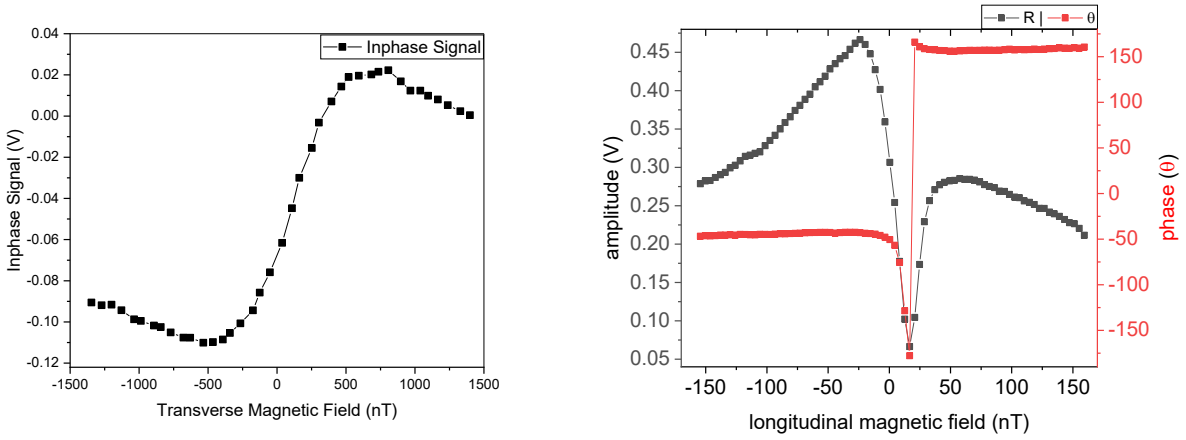

Figure 2. The Evolution of Longitudinal and Transverse Polarization Components of Probe Light and Zero Field Finding in Longitudinal Direction.

by applying longitudinal Hanle by means of a function generator and sweeping the transverse magnetic field by a lock-in amplifier simultaneously. Thus, the residual magnetic field in transverse direction was obtained and compensated by an additional power supply. Then, a longitudinal magnetic field with the magnitude of ~300 nT and 2 Hz frequency was applied in the presence of zero crossing transverse magnetic fields, and the variations were recorded in the amplitude of the longitudinal Hanle effect. As shown in Figure 3, the minimum point represents the residual magnetic field in the transverse direction. Further, another transverse component of the residual magnetic field was compensated by utilizing this method.

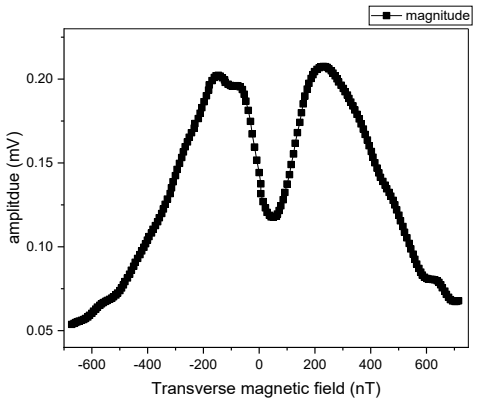

Figure 3. Compensation of the Residual Magnetic Field in Transverse Direction.

The data were collected after these measurements were performed in different temperatures. The width of the Hanle curve was compared before and after compensation (Figure 4).

The residual magnetic field has a destructive effect on FWHM of the curves, which increases by increasing the temperature (Figure 4). Furthermore, the Hanle curve damps in higher temperatures allow us to obtain a suitable Hanle effect due to the residual magnetic fields and compensation method. In addition, the dependency of the Hanle curve to the cell temperature indicates that the amplitude of the resonance curve (i.e. the sensitivity) increases by increasing the temperature while it decreases in higher temperatures due to residual magnetic fields in an unshielded environment.

Now, after efficient calibration, the sensitivity of the setup should be increased for distinguishing any heart defect. To this aim, the laser frequency was swept and the amplitude of the Hanle curve was recorded simultaneously to find the absorption line associated with the maximum of Hanle response. Thus, the peaks on the curve are the best alternative for laser operating frequency to have the

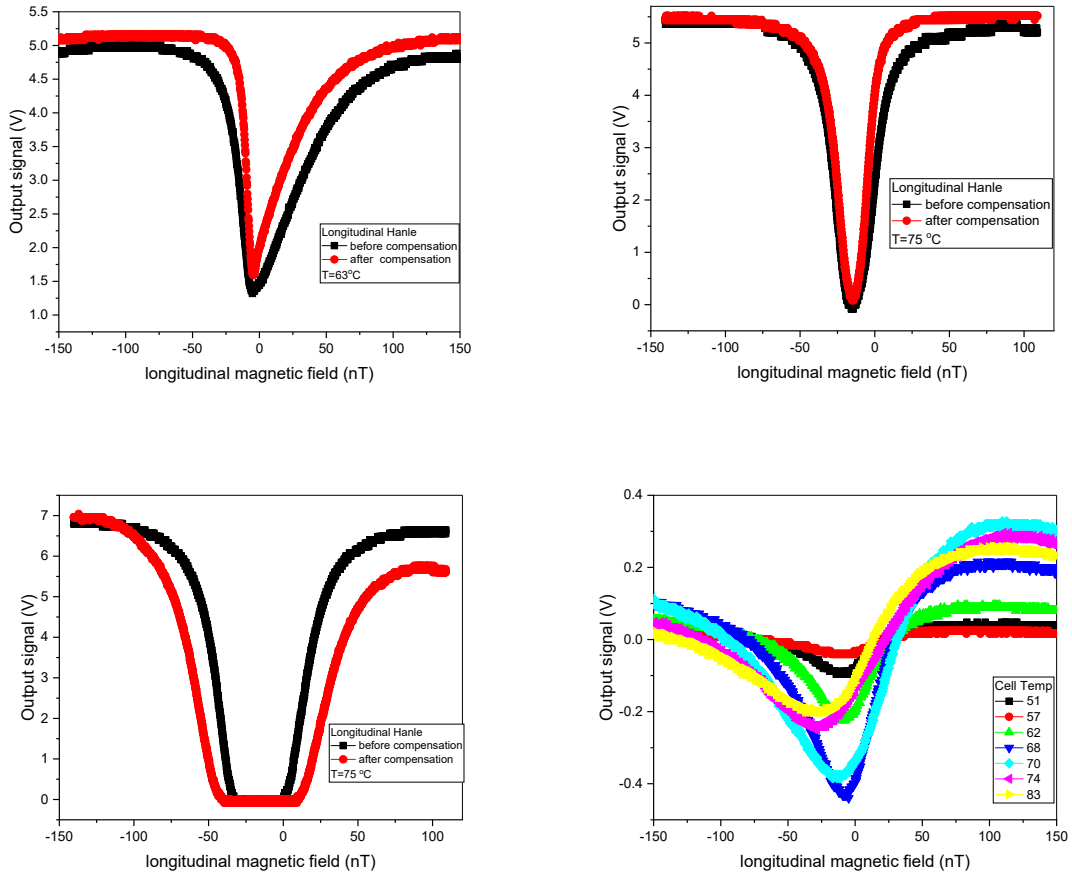

Figure 4. The Effect of Residual Magnetic Field Compensation on Hanle Curve in Different Temperatures and Residual Field Destructive Effect on Resonance Curve in High Temperatures.

best magnetometer response. As shown in Figure 5, the D1 laser was tuned to the F=2 to F'=1 hyperfine transition of ^{87}Rb to obtain the best output signal.

Results

Myocardial Ischemia Detection by Optimized Setup

Figure 1 shows the measurement of the changes of the residual magnetic field in the probe beam. Measuring weak magnetic fields was possible by enhancing the sensitivity. An MCG trace of a human's heart was simulated and applied through the current of transverse coils around the cell after optimizing the cell temperature, laser frequency, and residual magnetic field. The simulation was performed by utilizing a programmable function generator which could produce an arbitrary voltage. Figure 6 displays the applied normal MCG trace with the amplitude of 100 pT and the smoothed output signal of the magnetometer. As shown, the MCG data obtained with the atomic magnetometer allows distinguishing the QRS complex and T-wave as the typical features.

The MCG traces of different stages of myocardial ischemia disease were simulated by the transverse coils, and the smoothed output signal was measured (Figure 7).

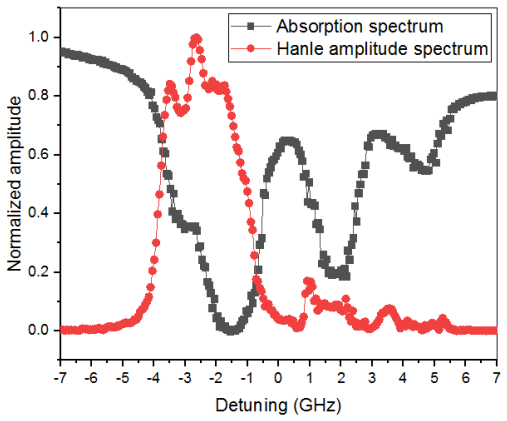

Figure 5. Variation of Hanle Amplitude Versus Laser Frequency Sweeping.

As shown, the T-wave turned upside down and the rest parts of the MCG trace remained intact. The output trace is presented in Figure 7 (a) as T-wave inversion. The emersion of injury at the ischemic area results in changing ST segment as displayed in Figure 7 (b). The appearance of infraction in the zone of injury is considered the third step. The effect of this infraction on the MCG trace was simulated and applied through Helmholtz coils. Figure 7(c) shows the output trace of the infraction. According to the healing process of Ischemia, the MCG trace returns to normal condition (Figure 6) after eliminating injury at the Ischemic zone.

Discussion

The MCG data changed as a consequence of the myocardial ischemia. Myocardial ischemia occurs when blood flow to the heart muscle is obstructed by a partial or complete blockage of a coronary artery by a buildup of plaques. Ischemia leads to some changes in the ST segment and T-wave. The ST segment may be either elevated or depressed. The T-wave may decrease in amplitude (flat T-waves), become negative (T-wave inversion), or even increase in amplitude (hyperacute T-wave). The temporal and spatial distribution of the human cardiac magnetic field should be recorded for observing the local magnetic signature of myocardial ischemia.

Consequently, in this study, we developed a human MCG system based on an atomic magnetometer with field sensitivity around 5 pT/Hz$^{1/2}$. This system consists of three pairs of Helmholtz coils for compensating the Earth's magnetic field and a single atomic magnetometer which could be utilized as one channel of a multi-channel MCG system, accompanied by a computer for acquiring and processing the signals. The MCG signals are recorded on the body surface of the patients. The results demonstrated the feasibility of the Hanle-based atomic magnetometer for utilizing in multi-channel configuration and performing MCG measurements such as prevention, diagnosis, and

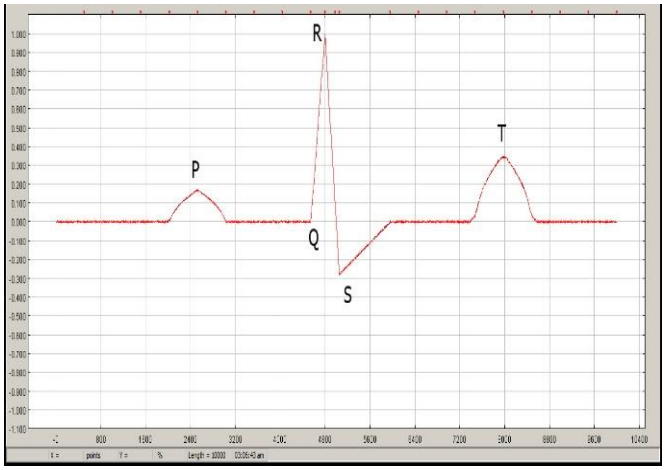

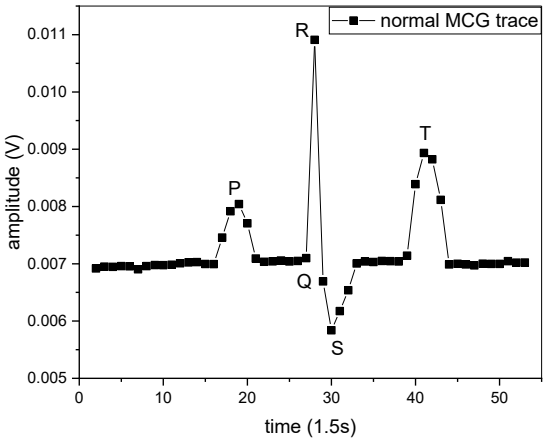

Figure 6. Normal MCG Trace of the Human Heart.

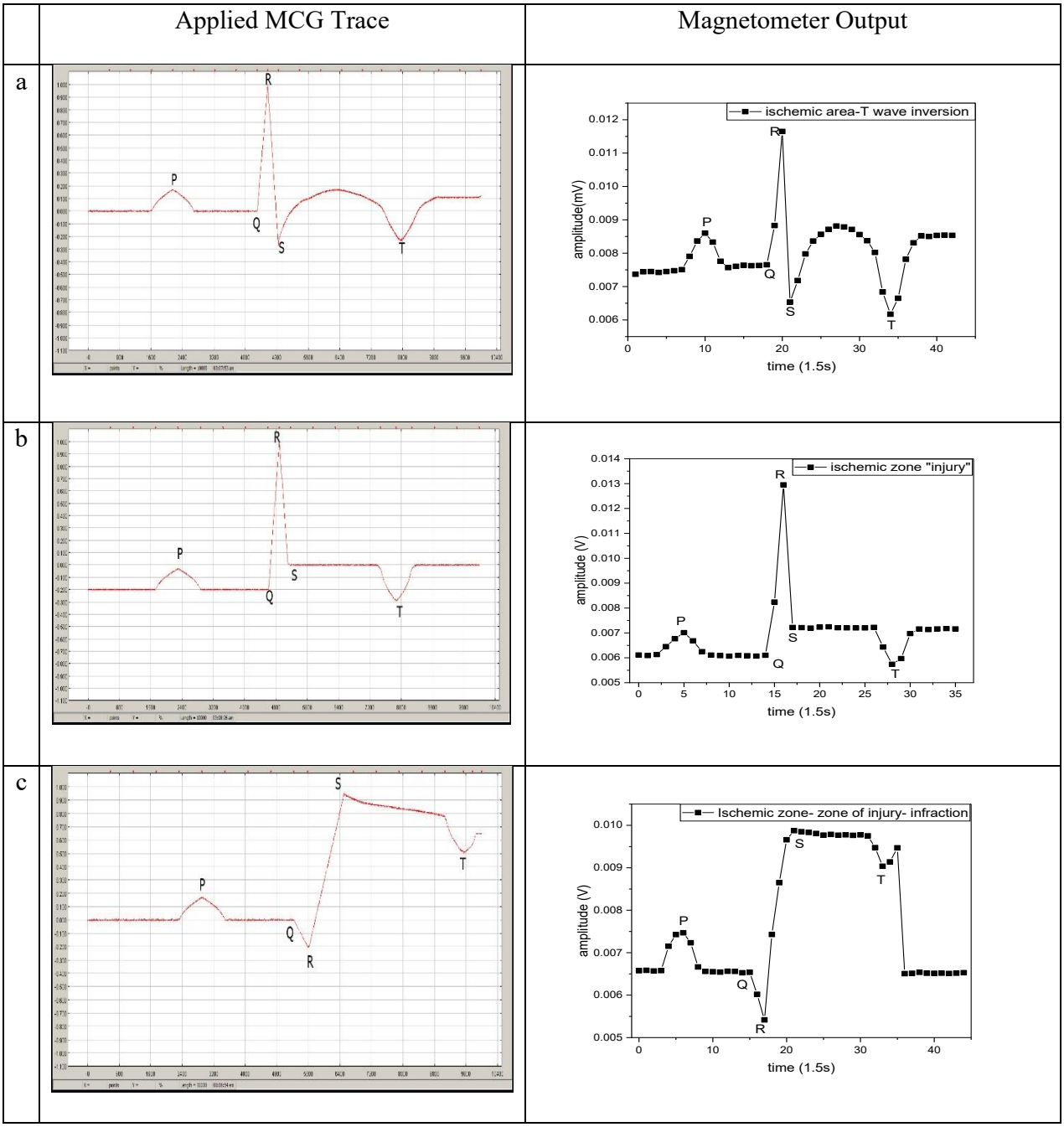

Figure 7. Three Stages of the Myocardial Ischemia MCG Trace.

treatment of heart diseases. This technique plays a role in diagnosing epilepsy, cardiac arrhythmias, coronary artery diseases like myocardial ischemia, heart attacks, angina, peripheral artery disease, and aortic stenosis.

In similar studies, MCG traces recorded by different channels have been converted to magnetic field maps in order to visualize the distribution of biomagnetic fields. Wylllie et al presented a portable four-channel atomic magnetometer array operating in the spin exchange relaxation-free (SERF) regime by obtaining the sensitivity of $11 fT/\sqrt{Hz}$.[9] In this regime, the spin-exchange collisions were greatly suppressed by working in the near-zero magnetic field and high Rb vapor temperature. However, in our Hanle-based magnetometers, it was necessary to zero the residual magnetic field, while the Rb cell temperature was not as high as the SERF regime.

In another study, Yang et al. developed a wearable multichannel human MCG system based on a SERF regime magnetometer array reliable for detecting MCG signals which could provide cardiac electromagnetic activity imaging.[8] However, MCG signals in ischemic condition have less been emphasized in these systems. Shifting our system to a multichannel gradiometer working in the SERF regime can increase the sensitivity

to $aT/\sqrt{Hz}$. However, residual noise, setup integration, and auto-calibration of the system can be considered as some of the limitations of future work. Moreover, the multi-channel configuration of the magnetometers could facilitate the treatment process and increase the sensitivity of disease diagnosis.

Conclusion

Recently, atomic magnetometers have shown promise for utilization in magnetocardiographic systems. To investigate the feasibility of the magnetometers in detecting heart diseases like myocardial ischemia, laser-pumped atomic magnetometers were presented by employing a pump-probe setup which can be used for recording two-dimensional cardio-magnetic signals. The presented method could detect the simulated P, QRS, and T heart features successfully. Based on the results, the method can represent enough sensitivity compared with other magnetometers, and the calibration of adjustable characteristics of the magnetometer can improve the sensitivity of the measurements. The results of this study can be useful for magnetocardiographic systems operating in an unshielded environment.

Authors' Contribution

AZ conceived the application of atomic Hanle magnetometer in the detection of simulated MCG signal in ischemic condition. Also, he performed the experiments and wrote the main text of the manuscript. MR designed and fabricated the atomic magnetometer and wrote the text of the manuscript. SMHK and SMH assisted in the laboratory setting and preparation of the article and MMT supervised and directed the research. All authors discussed the results and commented on the manuscript.

Conflict of Interests

The authors declare that they have no conflict of interest.

Ethical Considerations

Not applicable.

Funding

This research was supported by the Cognitive Sciences and Technologies Council of Iran under Grant number 3655.

References

1. Watanabe S, Yamada, S. Magnetocardiography in Early Detection of Electromagnetic Abnormality in Ischemic Heart Disease. *J Arrhythm*. 2008;24(1):4-17. doi: 10.1016/S1880-4276(08)80002-6.
2. Sheldon TJ, Stylos L, Nelson SD, Stadler RW, inventors; Medtronic Inc, assignee. Ischemia detection. *USPTO.* No. 6,937,899. August 30, 2005.
3. Alday E, Ni H, Zhang C, Colman M, Gan Z, Zhang H. Comparison of Electric- and Magnetic-Cardiograms Produced by Myocardial Ischemia in Models of the Human Ventricle and Torso. *PLoS One*. 2016; 11(8):e0160999. doi: 10.1371/-journal.pone.0160999.
4. Park J, Jung F. Qualitative und quantitative Beschreibung von myokardialen Ischämien mittels Magnetokardiographie / Qualitative and Quantitative Description of Myocardial Ischemia by means of Magnetocardiography. *Biomed Tech (Berl)*. 2004; 49(10): 266-272. doi: 10.1515/bmt.2004.050.
5. Bick M, Sternickel K, Panaitov G, Effern A, Zhang Y, Krause H, SQUID gradiometry for magnetocardiography using different noise cancellation techniques. *IEEE Trans Appl Supercond*. 2001;11(1):673-676. doi: 10.1109/77.919434.
6. Li H, Zhang S, Zhang C, Xie X. SQUID-Based MCG Measurement Using a Full-Tensor Compensation Technique in an Urban Hospital Environment. *IEEE Trans Appl Supercond*. 2016; 26(6):1-5. doi: 10.1109/TASC.2016.2569507.
7. Robbes D. Highly sensitive magnetometers a review. *Sens Actuator A Phys*. 2006; 129(1-2): 86-93.doi: 10.1016/j.sna.2005.11.023.
8. Yang Y, Xu M, Liang A, Yin Y, Ma X, Gao Y, et al. A new wearable multichannel magnetocardiogram system with a SERF atomic magnetometer array. *Sci Rep*. 2021; 11(1):5564. doi: 10.1038/s41598-021-84971-7.
9. Wyllie R, Kauer M, Smetana G, Wakai R, Walker T. Magnetocardiography with a modular spin-exchange relaxation-free atomic magnetometer array. *Phys Med. Biol*. 2012; 57(9):2619-2632. doi: 10.1088/0031-9155/57/9/2619.
10. Eswaran H, Escalona-Vargas D, Bolin E, Wilson J, Lowery C. Fetal magnetocardiography using optically pumped magnetometers: a more adaptable and less expensive alternative?. *Prenat. Diagn*. 2017; 37(2): 193-196. doi: 10.1002/pd.4976.
11. Bell W. and Bloom A, Optical Detection of Magnetic Resonance in Alkali Metal Vapor. *Phys Rev.* 1957;107(6):1559-1565. doi: 10.1103/PhysRev.107.1559.
12. Dang H, Maloof A, Romalis M. Ultrahigh sensitivity magnetic field and magnetization measurements with an atomic magnetometer. *Appl Phys Lett*. 2010; 97(15):151110. doi: 10.1063/1.3491215.
13. Kiwoong Kim, Won-Kyu Lee, In-Seon Kim and Han Seb Moon, Atomic Vector Gradiometer System Using Cesium Vapor Cells for Magnetocardiography: Perspective on Practical Application. *IEEE Trans Instrum Meas*. 2007; 56(2): 458-462. doi: 10.1109/TIM.2007.-890610.
14. Fenici R, Mashkar R. Brisinda D. Performance of miniature scalar atomic magnetometers for magnetocardiography in an unshielded hospital laboratory for clinical electrophysiology. *Eur Heart J*. 2020; 41(Supplement 2): ehaa946.0386. doi: 10.1093/ehjci/-ehaa946.038.